

Efficient on-chip source of microwave photon pairs in superconducting circuit QED

Florian Marquardt

Physics Department, Center for NanoScience, and Arnold Sommerfeld Center for Theoretical Physics,
Ludwig-Maximilians-University Munich, Theresienstr. 37, 80333 Munich, Germany

We describe a scheme for the efficient generation of microwave photon pairs by parametric down-conversion in a superconducting transmission line resonator coupled to a Cooper pair box serving as an artificial atom. By properly tuning the first three levels with respect to the cavity modes, the down-conversion probability may become higher than in the most efficient schemes for optical photons. We show this by numerically simulating the dissipative quantum dynamics of the coupled cavity-box system and discuss the effects of dephasing and relaxation. The setup analyzed here might form the basis for a future on-chip source of entangled microwave photons.

Introduction. –The generation of photon pairs by parametric down conversion (PDC) [1, 2, 3, 4, 5] represents one of the basic ways to create nonclassical states of the electromagnetic field, which has found numerous applications so far. The conditional detection of one of the photons enables the production of single photon Fock states [2, 6]. Furthermore, PDC is the primary method to generate entangled pairs of particles. Apart from the possibility of testing Bell inequalities [3, 4, 5, 7], this represents a crucial ingredient for a multitude of applications in the field of quantum information science, ranging from quantum teleportation through quantum dense coding to quantum key distribution [8].

With the advent of superconducting circuit quantum electrodynamics [9, 10], it will now be possible to take over many of the concepts that have been successful in the field of quantum/atom optics and transfer them to the domain of microwave photons guided along coplanar waveguides on a chip, interacting with superconducting qubits [11, 12, 13, 14]. Recent experiments have realized the strong-coupling limit of the Jaynes-Cummings model known in atom optics, employing a superconducting qubit as an artificial two-level atom, and coupling it resonantly to a harmonic oscillator (i.e. a cavity mode [10] or a SQUID [15]). Dispersive QND measurements of the qubit state, Rabi oscillations and Ramsey fringes have been demonstrated [16, 17], leading to a fairly detailed quantitative understanding of the system, which behaves almost ideally as predicted by theory [9].

In this paper, we will analyze a scheme that implements parametric down-conversion of microwave photons entering a transmission line resonator coupled to a Cooper pair box (CPB) providing the required non-linearity (Fig. 1). This represents the limit of a single artificial atom taking the place of the nonlinear crystal usually employed in optical PDC experiments [1, 2, 3, 5], with the cavity enhancing the PDC rate (cf. [18]). In contrast to other solid state PDC proposals [19, 20, 21], both the basic cavity setup and the possibility of ejecting the generated photons into single-mode transmission lines with a high degree of reliability are already an experimentally proven reality [10, 16, 17]. Recently, squeezing

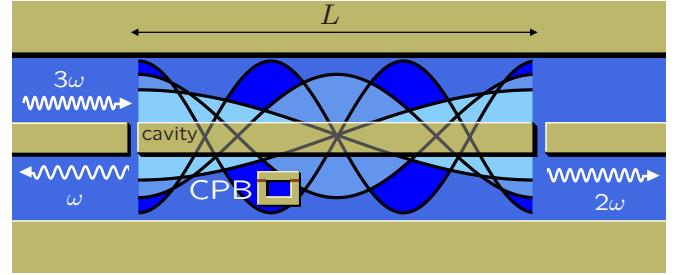


Figure 1: (color online) Schematic setup for the proposed parametric-down conversion (PDC) experiment in superconducting circuit cavity electrodynamics, with a Cooper-pair box (CPB) interacting with the three lowest modes of a transmission line resonator, whose voltage distributions are shown.

and degenerate parametric down-conversion have been analyzed theoretically [22] for a circuit QED setup coupling a charge qubit to two cavity modes. However, unlike the experiments and most of the theoretical investigations mentioned above, in this paper we propose to go beyond the regime where the box may be regarded as a two-level system (qubit), making use of its first three levels. By further employing its advantage over real atoms, namely its tunability via the applied magnetic flux and the gate voltage, this enables us to bring the transitions between the first three box levels into (near) resonance with the first three cavity modes (Fig. 2), thereby drastically enhancing the resulting probability of (nondegenerate) parametric down-conversion [23, 24, 25]. This represents the major advantage of the present scheme. We treat the full quantum dissipative dynamics of the box-cavity system, incorporating the radiation of photons from the cavity as well as nonradiative decay processes and dephasing in the CPB. We will present results for the down-conversion efficiency, discuss the minimization of unwanted loss processes, and comment on possible applications in the end.

The model. –The CPB is a device [14] in which Cooper pairs can tunnel between two superconducting islands due to a Josephson-coupling E_J (tunable by an external magnetic flux in a split-junction geometry). The number

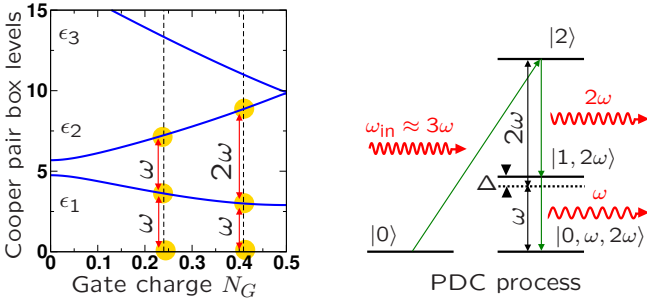


Figure 2: (color online) Left: Energy-level diagram of the CPB – transition energies in units of E_C , for $E_J = E_C = 3$, as a function of gate charge N_G . At particular gate values (away from the “qubit” regime near $N_G = 1=2$), the CPB transitions frequencies are related in an integer ratio, $(\epsilon_2 - \epsilon_1) = \epsilon_1 = 1:1$ or $2:1$, respectively. This enables to match them with the cavity modes, giving rise to particularly efficient degenerate or non-degenerate PDC ($2! \nabla ! + !$ or $3! \nabla ! + 2!$, respectively). Right: Simplified transition scheme for the non-degenerate PDC process considered in the text, with a detuning of the intermediate state $|j; 2! i$: $\epsilon_1 = ! +$.

of transferred Cooper pairs \hat{N} determines the charging energy, whose scale $E_C = e^2/2C$ is set by the total capacitance of the box island, and which can be controlled by application of an external gate voltage (expressed in terms of a gate charge N_G):

$$\hat{H}_{CPB} = 4E_C (\hat{N} - N_G)^2 + \frac{E_J}{2} \sum_N |N\rangle \langle N| + i c_N \hat{N} |j\rangle \langle j| + h.c. \quad (1)$$

Here $|N\rangle$ represents a charge state of the CPB. Two gaps in a superconducting coplanar waveguide act as mirrors of a cavity for microwave photons, $\hat{H}_{cavity} = \sum_{j=1}^3 \omega_j \hat{a}_j^\dagger \hat{a}_j$, where we will focus attention on the three lowest-lying cavity modes with $\omega_j = j!$ (we set $\omega_1 = 1$). The electric field inside the cavity acts on the CPB via a capacitive coupling, adding a fluctuating quantum-mechanical component to the gate charge N_G . This results [9] in an interaction

$$\hat{H}_{int} = \sum_{j=1}^3 \frac{X^3}{4} g_j (\hat{a}_j + \hat{a}_j^\dagger)^5 \hat{N} \quad (2)$$

The coupling constants (vacuum Rabi frequencies) $g_j = g_0 \int_0^L \psi_j(x) dx$, with $g_0 = 2 \frac{eC_A}{C} \omega_1 = L C_A$, are given in terms of the mode functions $\psi_1(x) = \sin(x/L)$, $\psi_2(x) = \cos(2x/L)$ and $\psi_3(x) = \sin(3x/L)$, which are defined on the interval $x = 0 \dots L=2 \dots L=2$.

The full Hamiltonian forming the basis of our analysis is thus given by

$$\hat{H} = \hat{H}_{cavity} + \hat{H}_{CPB} + \hat{H}_{int} + \hat{H}_{env} = \hat{H}_0 + \hat{H}_{env}; \quad (3)$$

where \hat{H}_{env} includes the coupling to the various reservoirs forming the environment. This involves both the possibility for microwave photons to leak out of the cavity, as well as the various possible nonradiative decay and decoherence processes acting on the CPB. The details will be specified below when setting up the master equation.

Basic considerations. – At least three basic features distinguish such a setup from the usual optical photon PDC experiments employing nonlinear crystals: (i) There is no momentum conservation, as the system is essentially zero-dimensional. (ii) However, energy conservation is much more restrictive, as the set of possible frequencies is limited to the discrete cavity modes. For appropriate input frequency, this results in a resonant enhancement of the PDC process. In contrast to a passive

filtering scheme, the bandwidth of the generated photons is reduced without diminishing the signal intensity. (iii) The microwave polarization is fixed and thus cannot be used for entanglement. At the end of this paper we will point out other options that can be explored.

Estimating the PDC rate. – If the CPB is operated as a two-level system (qubit) [22], the decay of a $3!$ photon into two lower-energy photons comes about through multi-step transitions, where at least one of the intermediate virtual states will have an energy detuning of the order of $!$, which contributes a small factor $(g/!)^2$ to the PDC rate.

However, we can enhance the PDC rate by exploiting more than the first two levels of the CPB. Indeed, by properly tuning the Josephson coupling E_J and the gate charge N_G , it is possible to make the transitions between the first three CPB energy levels $|j! i$, $|j! i$, $|j! i$ resonant with the cavity modes. The PDC process we want to consider is thus $|j; 3! i \nabla |j! i \nabla |j! i$, with $j = 3!$ and $j_1 = ! +$, such that all the transitions are (nearly) resonant. This reduces the largest energy denominator to the detuning $!$, resulting in an enhancement of the PDC rate by a factor of $(! =)^2$. What limits the enhancement? If $!$ is made too small, one may end up with less than a complete pair of down-converted photons: Instead of passing virtually through the intermediate state $|j; 2! i$ containing a $2!$ -photon and the CPB in its first excited level, that state will acquire a significant real population. As a result, the temporal correlation between photons would be destroyed, and nonradiative decays $|j; 2! i \nabla |j! i$ may occur, without emitting the second photon of frequency $!$. Clearly, there is a tradeoff between the achieved PDC probability and the fidelity of down-conversion. This will be confirmed by the detailed simulations below.

We will find that it is possible to achieve a PDC probability in the percent range that surpasses that of the most efficient modern optical PDC schemes [23] (which have a PDC probability of about 10^{-4} ; though the absolute PDC rate in those experiments is about 10^9 times larger due to the drastically higher input power). Earlier well-

known optical PDC experiments[5] generated less than one usable coincidence detection event for every 10^{13} incoming photons.

Simulation of the quantum-dissipative dynamics. – In the ideal case, one could integrate out the intermediate state, yielding an effective PDC term of the form $j\hat{a}_1^\dagger \hat{a}_2^\dagger + \text{h.c.}$. However, here we take into account all loss processes, by solving for the full dynamics of the CPB/cavity-system under an external microwave drive of frequency ω_{in} , using a Markov master equation of Lindblad form:

$$\frac{d\hat{\rho}}{dt} = (L_0 + L_{\text{drive}} + L_{\text{cavity}}^{\text{decay}} + L_{\text{CPB}}^{\text{relax}} + L_{\text{CPB}}^{\text{deph}})\hat{\rho} \quad (4)$$

Here $L_0\hat{\rho} = i[\hat{H}_0; \hat{\rho}]$, and the external microwave input, at a frequency ω_{in} and with an amplitude ϵ_1 , is described by $L_{\text{drive}}\hat{\rho} = i[\hat{H}_{\text{drive}}(t); \hat{\rho}]$, with $\hat{H}_{\text{drive}}(t) = \hat{a}_3^\dagger e^{i(\omega_{\text{in}}t + \phi)} + \text{h.c.}$

The dissipative terms in the Liouvillian are of Lindblad form

$$L[\hat{A}]\hat{\rho} = \hat{A}\hat{\rho}\hat{A}^\dagger - \frac{1}{2}\hat{A}^\dagger\hat{A}\hat{\rho} - \frac{1}{2}\hat{A}\hat{\rho}\hat{A}^\dagger \quad (5)$$

They describe: the decay of each cavity mode at a rate γ_j ($j = 1, 2, 3$),

$$L_{\text{cavity}}^{\text{decay}} = \sum_j \gamma_j L[\hat{a}_j]; \quad (6)$$

pure dephasing processes in the CPB that do not lead to transitions between levels (at rates γ_{ij}),

$$L_{\text{CPB}}^{\text{deph}} = \sum_{j < i} \gamma_{ij} L[\hat{a}_i^\dagger \hat{a}_j]; \quad (7)$$

and nonradiative relaxation processes leading from a level i to a lower energy level j of the qubit:

$$L_{\text{CPB}}^{\text{relax}} = \sum_{j < i} \gamma_{ij} L[\hat{a}_i^\dagger \hat{a}_j] \quad (8)$$

We keep only resonant terms ("rotating wave approximation", RWA) in the CPB-cavity interaction and go over to a frame rotating at ω_{in} , which eliminates the time-dependence in \hat{H}_{drive} , but replaces \hat{H}_0 by $\hat{H}_0 - \hat{W}$, with $3\hat{W} = \omega_{\text{in}} = \sum_j j\hat{a}_j^\dagger \hat{a}_j + j\hat{a}_1^\dagger \hat{a}_2 + 3j\hat{a}_2^\dagger \hat{a}_1$. This is accomplished by applying the time-dependent unitary transformation $\exp(i\hat{W}t)\hat{A}\exp(-i\hat{W}t)$ to the Hamiltonian $\hat{H}_0 + \hat{H}_{\text{drive}}$ and the density matrix.

We have obtained numerical solutions of the master equation for a wide range of parameters, and the results are shown in Figs. 3 and 5. All these simulations have been performed in a Hilbert space that has been truncated under the assumption of a small external drive

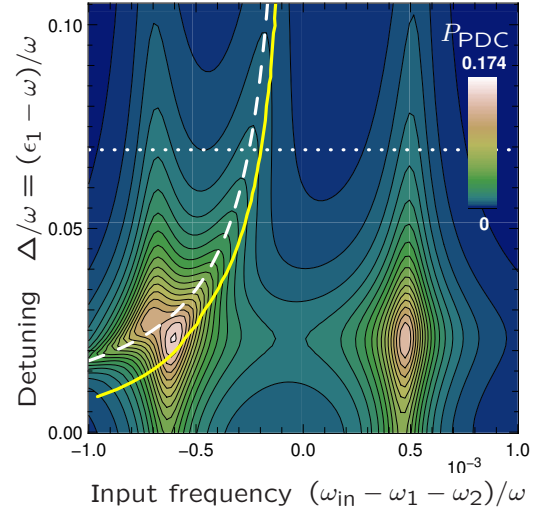


Figure 3: (color online) Parametric down-conversion probability $P_{\text{PDC}} = P(j; 2|i)^2 = j^2$, as a function of the microwave input frequency ω_{in} and the detuning of the intermediate state. The dashed line indicates the analytical resonance condition (see main text), the full line denotes the location of minimal Q_1 (high fidelity of PDC), and the dotted line is the cross-section shown in Fig. 4.

(The maximum excitation energy of the qubit+cavity system is restricted to $3\hbar$, and the down-conversion rate is linear in the input power). For the plots shown below, we have used experimentally reasonable parameter values: $g_0 = 10^{-2}$; $\gamma_j = 10^{-4}$; $\gamma_{ij} = 10^{-5}$ ($j < i$); $\gamma_{ij} = 2 \cdot 10^{-4}$ ($j > 0$). For reference, note that $\omega_{\text{in}} = 10$ GHz in typical experiments[10]. We have placed the CPB at $x = 0.3L$.

Discussion. – In order to interpret the results, we note that the production of photon pairs at a rate P_{PDC} is balanced by the decay of photons out of the cavity, at a rate γ . Thus, in an ideal lossless cavity PDC scheme, the probabilities to find the cavity in the states $|j; 2|i$, $|j|i$ and $|2|i$ all become equal to $P_{\text{PDC}} = (2\gamma)^{-1}$. Therefore, we define $P_{\text{PDC}} = (2\gamma)^{-1} P_{j; 2|i}$. The rate R of incoming photons is given by $R = 2j^2\gamma$. Thus, the PDC probability (chance of a given photon undergoing PDC) can be set to $P_{\text{PDC}} = P_{\text{PDC}}/R = P_{j; 2|i}^2 = j^2$ (we will use this as a definition even where the scheme deviates from ideal conditions, discussing the PDC fidelity separately).

In Fig. 3, we have plotted the PDC probability as a function of the input frequency ω_{in} and the detuning $\Delta = \omega_1 - \omega$. In general, P_{PDC} becomes maximal when ω_{in} matches the doublet frequencies ω_2 and $3\hbar$ (modified by the vacuum Rabi splitting): See the two vertical "ridges", independent of Δ . There is a third resonance at $\omega_{\text{in}} = 3\hbar - g_1^2/\omega$, with a dispersive shift depending on Δ , for which the input frequency matches the energy of the outgoing state (dashed curve). Here we have defined

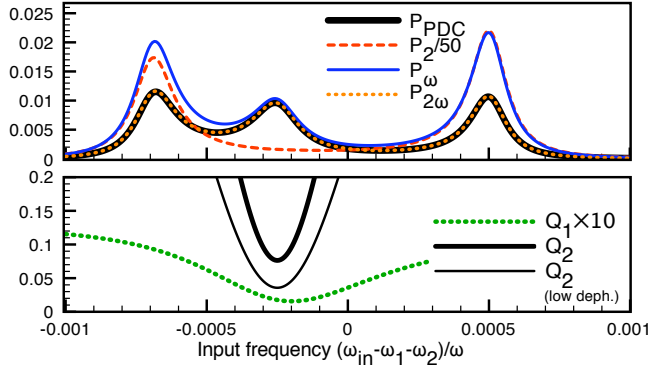


Figure 4: (color online) Top: The parametric down-conversion probability as a function of input frequency along the cross-section indicated in Fig. 3, and the probabilities $P_1 = \text{fP}(|j\rangle|i\rangle)$ and $P_2 = \text{fP}(|j\rangle|i\rangle)$ for one or two photons in the cavity, rescaled in the same manner, with $f = \omega^2/j^2$ (ideally $P_{\text{PDC}} = P_1 = P_2$). The probability of an excited qubit, $P_2 = \text{fP}(|j\rangle|i\rangle)$, is also shown. Bottom: The “non-ideality parameters” $Q_1 = P_{|j\rangle|2\rangle|i\rangle}/(P_{|j\rangle|2\rangle|i\rangle})$ and $Q_2 = P_{|j\rangle|i\rangle}/P_{|j\rangle|2\rangle|i\rangle}$, reaching a minimum at their idle peak (thin line: for half the dephasing rate of $\gamma = 2 \times 10^{-4}$).

$\hat{g}_1 = g_1 \hat{1} \hat{N} \hat{0}$ as the actual vacuum Rabi frequency. Although P_{PDC} becomes maximal when any of these resonances cross, this does not yield ideal photon pairs, as will become clear shortly. Turning to Fig. 4 (top), we see a cross-section of P_{PDC} (as a function of ω_{in}). In addition, we have included the probabilities of having one or two photons inside the cavity, which (in this normalization) should be identical to P_{PDC} in an ideal scheme. The apparent surplus in $|1\rangle$ -photons is due to a nonradiative process, as we will discuss now.

The relevant decay routes are: (i) $|j\rangle|i\rangle \rightarrow |j\rangle|i\rangle + |1\rangle|i\rangle$, (ii) $|j\rangle|2\rangle|i\rangle \rightarrow |j\rangle|i\rangle + |1\rangle|i\rangle$, (iii) $|j\rangle|2\rangle|i\rangle \rightarrow |j\rangle|i\rangle + |2\rangle|i\rangle$, and (iv) $|j\rangle|2\rangle|i\rangle \rightarrow |j\rangle|i\rangle + |1\rangle|i\rangle$. Process (i) leads to a single $|1\rangle$ photon being emitted, while (ii)–(iv) produce a single $|2\rangle$ photon with no corresponding partner photon. All of these processes get suppressed with an increasing energy mismatch $j = j_1 - |j|$ between the states $|j\rangle$ and $|j\rangle$. A larger broadening of the levels (produced by dephasing or decay) may partially overcome this energy mismatch, leading to a higher rate of unwanted loss processes. In order to quantify these processes, we have plotted, in Fig. 4 (bottom), the “non-ideality measures” $Q_1 = P_{|j\rangle|2\rangle|i\rangle}/(P_{|j\rangle|2\rangle|i\rangle})$ and $Q_2 = P_{|j\rangle|i\rangle}/P_{|j\rangle|2\rangle|i\rangle}$. Here Q_1 measures the ratio of nonradiative relaxation from the intermediate state $|j\rangle|2\rangle|i\rangle$ to the rate of pair emission, while Q_2 indicates the degree to which the populations of $|j\rangle|i\rangle$ and $|j\rangle|2\rangle|i\rangle$ are identical (which is the case ideally, for $j = j_1$). Both Q_1 and Q_2 should be as small as possible. The doublet peaks yield a large PDC rate, but also a large population of the CPB excited state $|j\rangle|i\rangle$, leading to the decay process (i) and a resulting surplus of

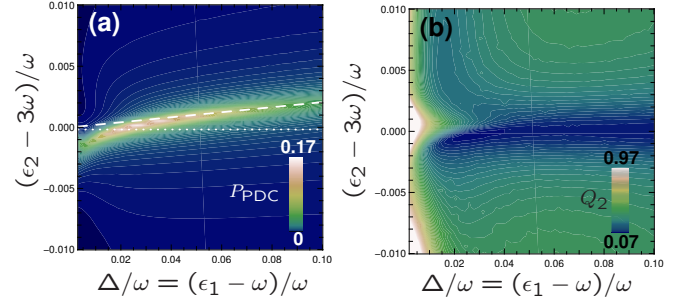


Figure 5: (color online) (a) Parametric down-conversion probability P_{PDC} , and (b) the non-ideality parameter Q_2 , as a function of the detunings between the Cooper-pair box energy levels $|1\rangle, |2\rangle$ and the cavity modes (controlled by E_J and N_G). At each point, the microwave input frequency ω_{in} has been chosen to minimize the parameter Q_1 (cf. Fig. 4). The dotted line indicates the cross-section displayed in Fig. 3.

$|1\rangle$ -photons (Fig. 4, top). Thus, we observe that the vacuum Rabi splitting of the doublet is essential: it allows for the appearance of the third (middle) peak in P_{PDC} that has a far lower qubit population and corresponding rate of unwanted loss processes (minimal in $Q_{1,2}$). Any reduction in the broadening of the peaks (set by γ ; γ) helps to further increase the quality of PDC.

The PDC quality can also be measured by evaluating the 2-photon correlator $K_{j1}(t) = \langle \hat{a}_1^\dagger \hat{a}_j^\dagger(t) \hat{a}_j(t) \hat{a}_1(t) \rangle = \langle \hat{a}_1^\dagger \hat{a}_1 \hat{a}_j^\dagger \hat{a}_j \rangle$; which determines the probability to detect a mode j photon at time t inside the cavity, provided a mode 1 photon has been detected at $t = 0$. Using the quantum regression theorem applied to our master equations, we have checked that at small values of $Q_{1,2}$, the ideal case is indeed observed, where the correlator decays at a rate γ , both for $(j;1) = (1;2)$ and $(j;1) = (2;1)$, while nonradiative processes change these decay rates and make them unequal.

The gate charge N_G and the Josephson coupling E_J change the relevant energies ϵ_1 and ϵ_2 of the first two excited states of the Cooper pair box, and, to a lesser degree, the matrix elements for the coupling to the cavity field. At a given value of E_J , one can tune to $N_G = N_G[E_J]$, such that the bare resonance condition $\epsilon_2 = 3\omega$ is fulfilled. In the following, we consider the effects of a small additional “offset gate charge” N_G , which mainly changes ϵ_2 , while E_J itself is used to tune ϵ_1 . The plots discussed so far have been obtained at fixed N_G , while changing E_J . At any given value of E_J and N_G , it is possible to select an input frequency ω_{in} which minimizes Q_1 . The resulting PDC rate has been plotted as a function of the detunings of the two CPB energy levels, ϵ_1 and ϵ_2 , in Fig. 5 (a), while the corresponding parameter Q_2 is shown in Fig. 5 (b) (Q_1 is below 0.01 in the relevant region where Q_2 is small).

We conclude that, while maintaining a good reliability

of the PDC process, the down conversion probability can become on the order of a few percent in the present setup, which thus indeed represents a highly efficient source of photon pairs. Similar results have been found for other reasonable parameter sets (e.g. $g_0 = 10^{-2}$; $j = 10^{-5}$; $j_{j=1} = 10^{-4}$ ($j < 1$); $j_{j=1} = 10^{-3}$ ($j > 0$)).

Generation of entanglement. – The down-converted $1!$ and $2!$ -photons can independently leak out of either side of the cavity. By post-selecting (cf. [3, 24]) only events where a photon is detected both in the left and the right arm each, one ends up with a frequency-entangled state that is directly equivalent to the entangled triplet state: $|2! i_L\rangle |j! i_R\rangle + |j! i_L\rangle |2! i_R\rangle$. We note, however, that a full Bell test requires measurements in a superposition basis, which is hard to realize for states of different energies.

Another, simpler, possibility is to test for energy-time entanglement as first proposed by Franson [4, 7, 25]. This requires feeding the generated photons into Mach-Zehnder interferometers, each of them containing a short and a long arm as well as a variable phase-shifter in one of the arms. By measuring the photon-detection correlation between the altogether four output ports of the two interferometers, it is possible to violate the usual kinds of Bell inequalities. The great advantage of such a scheme (particularly in the context of superconducting circuit QED) is that it does not require the polarization as a degree of freedom.

A less demanding, first experimental test of the PDC source described here might measure the intensity cross-correlations of the microwave output beams ($1!$ and $2!$) or implement homodyning techniques [6, 26] to characterize the quantum state. Finally, it is worth noting that for $j_3 = 2$ a sufficiently strong vacuum Rabi splitting between $|j! i\rangle$ and $|j! i\rangle$ in principle enables a scheme where a Rabi pulse is used to put exactly one excitation into the system, which then decays in the way described here, thus realizing a source of microwave photon pairs on demand.

Conclusions. – In this paper we have described and analyzed a setup for parametric down conversion in superconducting circuit cavity QED, suitable for the generation of pairs of entangled microwave photons. In contrast to earlier discussions, we have considered employing a transition via the first three levels of the artificial atom (Cooper pair box), which can be tuned to achieve a drastically enhanced PDC rate. We have analyzed the trade-off between optimizing the PDC rate and minimizing loss processes, by carrying out extensive numerical simulations of the quantum dissipative dynamics. The setup described here can be realized by moderate modifications of existing experiments, and it can hopefully form the basis for more detailed investigations into the nonclassical properties of the microwave field in circuit QED experiments.

Acknowledgments. I thank S. Girvin, A. Wallraff, A. Blais, J. Majer, D. Schuster, M. Mariantoni, E. Solano and R. Schoelkopf for discussions, and especially M. H. Devoret for pointing out the potential use of a three-level configuration. This work was supported by the DFG.

-
- [1] D. C. Burnham and D. L. Weinberg, Phys. Rev. Lett. 25, 84 (1970).
 - [2] C. K. Hong and L. Mandel, Phys. Rev. Lett. 56, 58 (1986).
 - [3] Y. H. Shih and C. O. Alley, Phys. Rev. Lett. 61, 2921 (1988).
 - [4] J. Brendel, E. M. Ohler, and W. Martienssen, Europhys. Lett. 20, 575 (1992).
 - [5] P. G. Kwiat, K. Mattle, H. Weinfurter, A. Zeilinger, A. V. Sergienko, and Y. Shih, Phys. Rev. Lett. 75, 4337 (1995).
 - [6] A. I. Lvovsky, H. Hansen, T. Aichele, O. Benson, J. Mlynec, and S. Schiller, Phys. Rev. Lett. 87, 050402 (2001).
 - [7] P. R. Tapster, J. G. Rarity, and P. C. M. Owens, Phys. Rev. Lett. 73, 1923 (1994).
 - [8] C. H. Bennett and D. P. DiVincenzo, Nature 404, 247 (2000).
 - [9] A. Blais, R. S. Huang, A. Wallraff, S. M. Girvin, and R. J. Schoelkopf, Phys. Rev. A 69, 062320 (2004).
 - [10] A. Wallraff, D. I. Schuster, A. Blais, L. Frunzio, R. S. Huang, J. Majer, S. Kumar, S. M. Girvin, and R. S. Schoelkopf, Nature 431, 162 (2004).
 - [11] V. Bouchiat, D. Vion, P. Joyez, D. Esteve, and M. H. Devoret, Physica Scripta T 76, 165 (1998).
 - [12] Y. Nakamura, Y. A. Pashkin, and J. S. Tsai, Nature 398, 786 (1999).
 - [13] J. E. Mooij, T. P. Orlando, L. Levitov, L. Tian, C. H. van der Wal, and S. Lloyd, Science 285, 1036 (1999).
 - [14] Y. Makhlin, G. Schon, and A. Shnirman, Rev. Mod. Phys. 73, 357 (2001).
 - [15] I. Chiorescu, P. Bertet, K. Semba, Y. Nakamura, C. J. P. M. Hamers, and J. E. Mooij, Nature 431, 159 (2004).
 - [16] D. I. Schuster et al., Phys. Rev. Lett. 94, 123602 (2005).
 - [17] A. Wallraff et al., Phys. Rev. Lett. 95, 060501 (2005).
 - [18] M. Oberparleiter and H. Weinfurter, Optics Communications 183, 133 (2000).
 - [19] O. Benson, C. Santori, M. Pelton, and Y. Yamamoto, Phys. Rev. Lett. 84, 2513 (2000).
 - [20] O. Gywat, G. Burkard, and D. Loss, Phys. Rev. B 65, 205329 (2002).
 - [21] C. Emary, B. Trauzettel, and C. W. J. Beenakker, Phys. Rev. Lett. 95, 127401 (2005).
 - [22] K. Moon and S. M. Girvin, Phys. Rev. Lett. 95, 140504 (2005).
 - [23] K. Edamatsu, G. Ohata, R. Shimizu, and T. Itoh, Nature 431, 167 (2004).
 - [24] A. Aspect, J. Dalibard, and G. Roger, Phys. Rev. Lett. 49, 1804 (1982).
 - [25] J. D. Franson, Phys. Rev. Lett. 62, 2205 (1989).
 - [26] M. Mariantoni, M. J. Storz, F. K. Wilhelm, W. D. Oliver, A. Emmert, A. Marx, R. Gross, H. Christ, and E. Solano, cond-mat/0509737 (2005).